Distinguishing between s+id and s+is pairing symmetries in multiband superconductors through spontaneous magnetization pattern induced by a defect

Shi-Zeng Lin, Saurabh Maiti, and Andrey Chubukov

Distinguishing between $s + id$ and $s + is$ pairing symmetries in multiband superconductors through spontaneous magnetization pattern induced by a defect

Shi-Zeng Lin,[1] Saurabh Maiti,[2] and Andrey Chubukov[3]

[1]*Theoretical Division, Los Alamos National Laboratory, Los Alamos, New Mexico 87545, USA*
[2]*Department of Physics, University of Florida, Gainesville, FL-32611, USA*
[3]*Department of Physics, University of Minnesota, Minneapolis, Minnesota 55455, USA*

(Dated: August 9, 2016)

The symmetry of the pairing state in iron pnictide superconductor $Ba_{1-x}K_xFe_2As_2$ is still controversial. At optimal doping ($x \approx 0.4$), it is very likely s-wave, but for $x = 1$ there are experimental and theoretical arguments for both s-wave and d-wave. Depending on the choice for $x = 1$, intermediate $s + is$ and $s + id$ states have been proposed for intermediate doping $0.4 < x < 1$. In both states, the time reversal symmetry is broken and a spontaneous magnetization is allowed. In this work we study a spontaneous magnetization induced by a nonmagnetic defect in the $s+is$ and $s+id$ states by using a perturbation theory and numerical calculations for the Ginzburg-Landau free energy functional. We show that the angular dependence of the magnetization is distinct in these two states due to the difference in symmetry properties of the order parameters. Our results indicate a possible way to distinguish between the $s + is$ and $s + id$ pairing symmetries in multi-band superconductors.

PACS numbers: 74.20.Rp, 74.20.Mn, 74.25.Jb, 76.75.+i

I. INTRODUCTION

The knowledge of the pairing symmetry of an unconventional superconductor is the first step to elucidate the pairing mechanism. In iron pnictide and iron-chalcogenide superconductors (FeSCs) the identification of the pairing symmetry is complicated by the following reasons. First, the family of iron-based superconductors is large, and it is not certain that the pairing symmetry is the same in all FeSCs. The two major candidates are s_{+-}[1–5] and $d_{x^2-y^2}$[2,5–8] states. At optimal doping s_{+-} state is favorable, but at larger hole doping several theoretical work suggested that s_{+-} and $d_{x^2-y^2}$ are almost degenerate[7,9,10]. Second, FeSCs are multi-band superconductors with several hole and electron Fermi pockets. The phase of s_{+-} gap changes by π between hole and electron pockets and the phase of $d_{x^2-y^2}$ gap changes by π between electron pockets. In general, however, multi-band superconductors allow more complex superconducting states with the phase differences of the gaps on different Fermi pockets as fractions of π.

These more complex superconducting states, even with pure $s-$wave symmetry, can be understood by noticing that the s_{+-} pairing symmetry originates from an interband repulsive interaction between superconducting condensates on hole and electron pockets. The intra-pocket repulsion favors a π phase shift in the superconducting order parameter. When three or more bands are present, the inter-band repulsion leads to frustration, which is resolved by choosing the phases of the gaps to maximize superconducting condensation energy. For example, for three identical pockets with equal repulsive interband interaction, the best outcome is the $\pm 2\pi/3$ difference between the phases of the three gaps, much like 120° spin configuration resolves frustration in an XY antiferromagnet on a triangular lattice. And just like there, the phase change can go in $2\pi/3$ ingredients clockwise or anticlockwise. The choice breaks the time reversal symmetry in addition to the overall phase $U(1)$ symmetry.[11–14] In a generic state of this kind, the order parameter $\hat{\Psi} \equiv (\Psi_1, \Psi_2, \Psi_3, ...)$ made out of $\Psi_i \equiv \Delta_i \exp(i\varphi_i)$ at a given Fermi pocket, and its complex conjugate $\hat{\Psi}^* \equiv (\Psi_1^*, \Psi_2^*, \Psi_3^*, ...)$ are not related by a global phase rotation, i.e., $\hat{\Psi} \neq \exp(i\theta_0)\hat{\Psi}^*$. Below we label such s-wave state as $s + is$.

The transition from a time-symmetry preserving s-wave state (e.g., s_{+-}) to an $s + is$ state is a continuous phase transition. Near the transition, a collective out-of-phase oscillation of φ_i (a Leggett mode) becomes soft.[15–17] Inside an $s+is$ state, the breaking of a discrete time reversal symmetry gives rise to a new kind of a phase soliton between the superconducting domains $\hat{\Psi}$ and $\hat{\Psi}^*$.[18–20] It has been proposed that one may detect the $s + is$ pairing symmetry based these properties.[15,19–26]

FeSCs with multiple Fermi surfaces are promising candidates for an $s + is$ state. The material $Ba_{1-x}K_xFe_2As_2$ is particularly interesting in this regard. It is magnetic at small x and superconducting at larger x. Its electronic structure for x not close to $x = 1$ consists of three hole pockets and two electron pockets. Near optimal doping, it is very likely that superconducting interaction is mediated by spin fluctuations. The magnetic order has the momentum equal to the distance between the centra of hole and of electron pockets, and fluctuations of this order clearly favor s_{+-} state without breaking the time-reversal symmetry and π phase shift between the gaps on hole and electron pockets. This is consistent with angle-resolved photoemission spectroscopy (ARPES) experiments, which near $x = 0.4$ found a fully gapped superconducting state with little variation of the gaps along the pockets.[27–31]. At $x = 1$, however, the situation is different: electron pockets disappear and only the hole pockets remain, according to the ARPES measurements.[32,33] If the pairing symmetry remains s-wave all the way to $x = 1$, as some ARPES[33] and penetration depth[34] measurements suggested, then the gap must change sign between inner and middle hole pockets, where the gaps are the largest, according to Ref. 33. The sign-changing s-wave gap structure was found in random phase approximation based theoretical studies for $x = 1$.[10] Two groups an-

alyzed[21,23] how the gap structure changes between s_{+-} state near optimal doping, with equal sign of the gaps on the hole pockets, and s-wave state at $x = 1$ with opposite signs of the gaps on the two smallest hole pockets. They found that the evolution is continuous near the T_c line, with the gap on one of hole pockets vanishing and re-appearing with a different sign as x approaches 1, but necessary involves an intermediate state at $T = 0$, when it is easier to change the phase of the order parameter rather than its amplitude. In this intermediate state, the phases of the gaps on the two smallest hole pockets differ by a fraction of π, i.e., the intermediate state is a realization of $s + is$ superconductivity.

Another suggestion, based on measurements of thermal conductivity, resistivity and temperature-dependent Raman spectra[8,35–38] and theoretical calculations using functional renormalization group[7], is that the pairing symmetry at $x = 1$ is a d-wave ($d_{x^2-y^2}$). This is also generally consistent with random phase approximation based calculations[10], which found that s-wave and $d_{x^2-y^2}$ couplings are almost degenerate. If so, the system must evolve from an s_{+-} superconductor at $x \sim 0.4$ to a d-wave superconductor at $x = 1$. Calculations show[39,40] that this evolution goes via an intermediate phase in which both s-wave and d-wave components are present, and the phase shift between the two is $\pm\pi/2$, i.e, the state is $s + id$. This is another state which breaks time-reversal pairing symmetry.

To summarize the experimental findings, there is arguments for both s-wave and d-wave gap symmetry in $Ba_{1-x}K_xFe_2As_2$ at $x \approx 1$. In both cases, theoretical reasoning shows that there must exist an intermediate phase with either $s+is$ or $s+id$ gap symmetry. Time reversal symmetry breaking has been probed in zero-field muon-spin relaxation studies of polycrystalline samples of $Ba_{1-x}K_xFe_2As_2$ with $0.5 \leq x \leq 0.9$ in Ref. 41 by searching for spontaneous currents, and so far such currents have not been found. We argue below that such negative result is inconsistent with the idea of $s+id$ state but does not actually rule out $s + is$ pairing symmetry.

In this work we discuss whether it is possible to distinguish between $s + is$ and $s + id$ states in experiments. Both states break time reversal symmetry and allow a spontaneous magnetization to develop. In a homogenous system, magnetization does not develop because a spontaneous current circulates in the band space and is not coupled to a gauge field. For instance, for a Josephson-like interband coupling, the interband supercurrent is $J_{ij} \propto \Delta_1\Delta_2 \sin(\varphi_1-\varphi_2)$, which is nonzero when $\varphi_1 - \varphi_2 \neq 0$ or π. The interband phase difference $\varphi_1 - \varphi_2$ does not couple to the vector potential, thus the spontaneous interband supercurrent does not induce magnetization. However, in the presence of nonmagnetic defects, a spontaneous current can be induced around the defect in superconductors with either $s + is$ or $s + id$ pairing symmetries[19,20,42,43]. Because the $s + id$ state breaks the lattice C_4 rotation symmetry, while the $s+is$ preserves it, the profile of the induced spontaneous magnetization are different for $s+is$ and $s+id$ states. This suggests a possible way to experimentally distinguish between the two pairing symmetries.

Below we report the results of our study on the spontaneous magnetization in $s + is$ and $s + id$ superconductors induced by nonmagnetic defects with different shapes. We extend the previous work[42,43] by developing a self consistent treatment for the magnetization based on a phenomenological Ginzburg-Landau free energy functional. Our results show that one can differentiate between the $s + is$ and $s + id$ states by measuring the magnetization pattern induced by nonmagnetic defects. We first present the symmetry argument to obtain the magnetization profile. We then present perturbative calculations of induced magnetization for a weak defect potential. We next compare the perturbative calculations with the numerical results obtained by minimizing the Ginzburg-Landau free energy functional. Finally, we compare our approach and the results to those in previous work.

II. MODEL AND PERTURBATIVE CALCULATIONS

A. Symmetry analysis

Before going into detailed calculations, let us first perform a symmetry analysis. The $s + is$ state has a full rotational symmetry. For a circular defect, if a supercurrent was induced, it could only flow inward or outward, as sketched in Fig. 1 (a). This would violate the current conservation $\nabla \cdot \mathbf{J}_s = 0$, hence no supercurrent (and no spontaneous magnetization) is allowed in this case. Consider next a square defect. Because x and y directions are equivalent, to conserve the supercurrent, the direction of the supercurrent along zone diagonals should be opposite to that in the x and the y directions. That is if the current flows inward in the x and the y directions, the current must flow outward in the diagonal direction, and vice versa. As a result, the induced magnetization, measured as a function of the angle with respect to, say, x direction, must display a four-fold oscillation [Fig. 1 (b)].

The $s + id$ state breaks the C_4 rotation symmetry and is invariant under the combination of the C_4 rotation and time reversal operation. In this situation, a supercurrent and a spontaneous magnetization do emerge, even if a defect is circular. For a circular or square defect, if the current in the x direction flows inward, then the current in the y direction must flow outward, and vice versa. The current conservation at the center of a defect is satisfied automatically. The magnetization pattern, generated by a supercurrent, displays a two-fold oscillation as a function of an angle [Fig. 1 (c) and (d)]. This simple analysis shows that one can indeed differentiate between an $s + is$ pairing state and an $s+id$ pairing state by analyzing the pattern of a spontaneous magnetization induced around a defect.

B. Ginzburg-Landau free energy

We next calculate a spontaneous magnetization induced by a defect using Ginzburg-Landau theory in two dimensions. We consider $s + is$ and $s + id$ states separately.
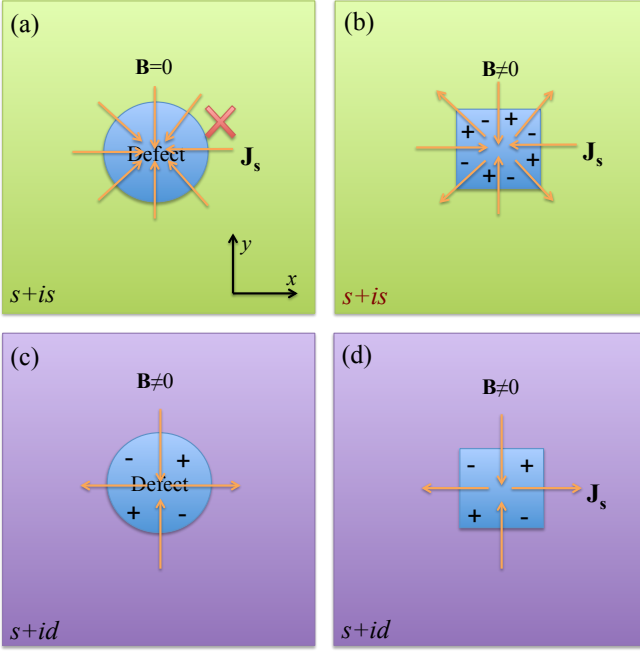
FIG. 1. (color online) Schematic view of the spontaneous supercurrent and magnetization induced by a circular and square defect in the $s + is$ and $s + id$ states based on the symmetry analysis. The arrows are the direction of supercurrent and $+(-)$ denotes the direction of the magnetization field perpendicular to the superconducting plane.

1. s + is state

Like we said, an $s + is$ state emerges when there are three (or more) Fermi pockets, due to frustration when inter-pocket interactions are repulsive.[12,21,23] However, recent work[44] has demonstrated that one can simplify the analysis of $s + is$ state by reducing the three-pocket model to an effective two-pocket model in which time reversal symmetry breaking is explicitly imposed. In this approach, which we follow, the Ginzburg-Landau free energy functional for an $s + is$ state is, up to terms of quartic order in Ψ_i:

$$\mathcal{F}\left(\Psi_i, \Psi_i^*\right) = \mathcal{F}_1 + \mathcal{F}_2 + \mathcal{F}_c + \frac{1}{8\pi}(\nabla \times \mathbf{A})^2, \qquad (1)$$

where the free energy density for each component Ψ_i is ($i = 1, 2$)

$$\mathcal{F}_i = \alpha_i |\Psi_i|^2 + \frac{\beta_i}{2}|\Psi_i|^4 + \frac{\hbar^2}{2m_i}\left|\hat{\mathbf{D}}\Psi_i\right|^2, \qquad (2)$$

and the coupling between Ψ_1 and Ψ_2 is described by

$$\mathcal{F}_c = \frac{\gamma_3}{2}|\Psi_1|^2|\Psi_2|^2 + \frac{\gamma_2}{2}\left[(\Psi_1^*\Psi_2)^2 + c.c.\right]$$
$$+\gamma_1\left(\Psi_1\Psi_2^* + c.c.\right) + \frac{\hbar^2}{4m_c}\left[\left(\hat{\mathbf{D}}\Psi_1\right)^* \cdot \hat{\mathbf{D}}\Psi_2 + c.c.\right], \qquad (3)$$

where $\hat{\mathbf{D}} = -i\nabla - 2\pi\mathbf{A}/\Phi_0$ and $\Phi_0 = hc/2e$ is the flux quantum. Because of competition between the bilinear and bi-quadratic terms (the γ_1 and the γ_2 terms), the phase difference between

Ψ_1 and Ψ_2 can be any value between 0 to 2π, and the exact value is determined by γ_1 and γ_2. The resulting state generally can be termed as $s + \exp(i\varphi)s$ state [for analogous consideration in coexistence state of superconductivity and magnetism, see Ref. 45]. To stabilize the $s+is$ state with a $\varphi = +\pi/2$ phase difference between Ψ_1 and Ψ_2, we set $\gamma_2 > 0$ and $\gamma_1 = 0$. For the $s + id$ case the γ_1 term is not allowed by symmetry.

A nonmagnetic defect is modeled by changing $\alpha_i \rightarrow \alpha_i + \tilde{\alpha}_i(r)$. A defect is considered as weak if the defect potential $\tilde{\alpha}_i \ll \alpha_i$. The variation of the order parameter $\Psi_i(r) = \Psi_{i0}[1 + \delta_i(r) + i\phi_i(r)]$, where Ψ_{i0} is the order parameters in the absence of defects, can be found from the minimization of the Ginzburg-Landau functional to linear order in $\tilde{\alpha}_i(r)$. The minimization obviously yields $\delta_i(r)$, $\phi_i(r) \propto \tilde{\alpha}_i(r)$. In a state with broken time-reversal symmetry an amplitude fluctuation $\delta_i(r)$ and a phase fluctuation $\phi_i(r)$ are coupled. As the consequence, a vector potential $\mathbf{A}(r)$ also fluctuates. Fluctuations of $\mathbf{A}(r)$ are gapped by Anderson-Higgs mechanism with the gap larger than that of collective excitations of $\delta_i(r)$ and $\phi_i(r)$, at least near the onset of a state which breaks time reversal symmetry.[15,16] To calculate $\delta_i(r)$ and $\phi_i(r)$ to the linear order in $\tilde{\alpha}_i(r)$, we fix the gauge by choosing the global phases such that $\mathbf{A} = \mathbf{0}$ when $\tilde{\alpha}(\mathbf{r}) = \mathbf{0}$. The resulting equations for δ_i and ϕ_i are presented in the Appendix. We assume that the defect potential $\tilde{\alpha}_i(\mathbf{r})$ has the angular dependence in the form $\tilde{\alpha}_i(\mathbf{r}) = \tilde{\alpha}_i(r)\cos(n\theta)$ and consider different integer n. The angular dependence of $\delta_i(r)$ and $\phi_i(r)$ follows that of $\tilde{\alpha}_i(\mathbf{r})$.

Minimizing next $\mathcal{F}$ with respect to $\mathbf{A}$, we obtain the Ampere's law

$$\nabla \times \nabla \times \mathbf{A} = \frac{4\pi}{c}\mathbf{J}_s, \qquad (4)$$

with the supercurrent

$$\mathbf{J}_s = \sum_i \frac{2e\hbar}{m_i}\left|\Psi_{i0}^2\right|(\nabla\phi_i + 2\delta_i\nabla\phi_i) - \frac{4e^2}{c}\sum_i \frac{\left|\Psi_{i0}^2\right|}{m_i}\mathbf{A}+$$
$$\frac{\hbar e}{m_c}|\Psi_{10}\Psi_{20}|(\nabla\delta_2 + \delta_1\nabla\delta_2 + \phi_1\nabla\phi_2 - \nabla\delta_1 - \delta_2\nabla\delta_1 - \phi_2\nabla\phi_1). \qquad (5)$$

The condition for current conservation, $\nabla \cdot \mathbf{J}_s = 0$, is satisfied automatically by Eq. (4). Taking $\nabla\times$ of both sides of Eq. (4) and using $\nabla \times \nabla\phi_i = 0$, which is valid as long as no vortices are present, we obtain

$$-\nabla^2\mathbf{B} + \lambda^{-2}\mathbf{B} = \frac{16\pi\hbar e}{c}\sum_i \frac{\nabla\delta_i \times \nabla\phi_i}{m_i}\left|\Psi_{i0}^2\right|$$
$$+\frac{8\pi\hbar e|\Psi_{10}\Psi_{20}|}{cm_c}(\nabla\delta_1 \times \nabla\delta_2 + \nabla\phi_1 \times \nabla\phi_2), \qquad (6)$$

where $\lambda^{-2} = 16\pi e^2 \sum_i \left|\Psi_{i0}^2\right|/(m_i c^2)$ is the London penetration depth (up to corrections of order δ_i). The induced magnetization is of second order in the defect potential $\tilde{\alpha}(r)$ and it is directed perpendicular the 2D superconductor plane.

For a model of a superconductor with identical $\Psi_{10} = \Psi_{20}$ and $m_1 = m_2$, $\delta_1(r) = \delta_2(r)$, and $\phi_1(r) = -\phi_2(r)$, the magnetization is absent because the right-hand side of Eq. (6)

vanishes. In a more generic case, using $\delta_i(\mathbf{r}) = \delta_i(r) \cos(n\theta)$ and $\phi_i(\mathbf{r}) = \phi_i(r) \cos(n\theta)$, we obtain the magnetization field

$$\mathbf{B}(r, \theta) = \hat{z} \sin(2n\theta) \int_0^\infty B(k) J_{2n}(kr) k \, dk, \quad (7)$$

where

$$B(k) = \frac{8\pi\hbar e n}{cr(k^2 + \lambda^{-2})} S(k), \quad (8)$$

and

$$S(k) = \int_0^\infty r \, dr J_{2n}(kr) \left[\sum_i \frac{2 \left| \Psi_{i0}^2 \right| (\delta_i \partial_r \phi_i - \phi_i \partial_r \delta_i)}{m_i} \right. $$
$$\left. + \frac{\delta_1 \partial_r \delta_2 - \delta_2 \partial_r \delta_1 + \phi_1 \partial_r \phi_2 - \phi_2 \partial_r \phi_1}{m_c} |\Psi_{10}\Psi_{20}| \right]. \quad (9)$$

The unit vector $\hat{z}$ is along the z direction, and J_{2n} is the Bessel function of the first kind. We see that a nonmagnetic defect with an n-fold angular variation $\tilde{\alpha}_i(r) = \tilde{\alpha} \cos(n\theta)$ induces a magnetization which displays a $2n$-fold oscillation: $B_z \propto \tilde{\alpha}^2 \sin(2n\theta)$. For a centrosymmetric defect potential $n = 0$, the induced magnetic field vanishes.

2. $s + id$ state

We proceed to study the magnetization pattern from a defect in an $s + id$ state. Let's denote an s-wave component by Ψ_1 and a d-wave component by Ψ_2. The Ginzburg-Landau free energy functional is still given by Eqs. (1) and (2), but the coupling term is different and is given by[42]

$$\mathcal{F}_c = \frac{\gamma_3}{2} |\Psi_1|^2 |\Psi_2|^2 + \frac{\gamma_2}{2} \left[(\Psi_1^* \Psi_2)^2 + c.c. \right]$$
$$+ \frac{\hbar^2}{4m_c} \left[\left(\hat{D}_x \Psi_1 \right)^* \hat{D}_x \Psi_2 - \left(\hat{D}_y \Psi_1 \right)^* \hat{D}_y \Psi_2 + c.c. \right]. \quad (10)$$

For the $s + id$ state, $\mathcal{F}$ is invariant under a rotation of a reference frame by $\pi/2$ and subsequent the time reversal operation, as both operations change the sign of a d-wave component Ψ_2. The γ_1 term in Eq. (3) is not invariant under the change of the sign of Ψ_2 and is not allowed. Note also that the mixed gradient terms in the x and the y directions must have different signs. We show below that, because of the mixed gradient term in Eq. (10), the magnetization is nonzero already to linear order in a defect potential.

To linear order in δ_i and ϕ_i, the supercurrent is

$$\mathbf{J}_s = \sum_i \frac{2e\hbar}{m_i} \left| \Psi_{i0}^2 \right| \nabla \phi_i - \frac{4e^2}{c} \sum_i \frac{\left| \Psi_{i0}^2 \right|}{m_i} \mathbf{A}$$
$$+ \left[\frac{\hbar e}{m_c} |\Psi_{10}\Psi_{20}| \left(\hat{x} \partial_x - \hat{y} \partial_y \right) (\delta_2 - \delta_1) \right], \quad (11)$$

where $\hat{x}$ and $\hat{y}$ are unit vectors in x and y directions, respectively. The magnetic field is determined by

$$-\nabla^2 \mathbf{B} + \lambda^{-2} \mathbf{B} = \frac{8\pi\hbar e |\Psi_{10}\Psi_{20}|}{cm_c} \hat{z} \partial_{x,y} (\delta_1 - \delta_2). \quad (12)$$
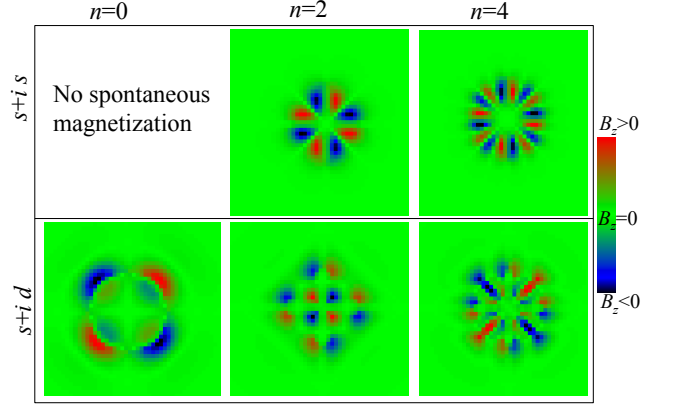

FIG. 2. (color online) Spontaneous magnetization induced by a weak defect with n-fold angular dependence in the $s + is$ and $s + id$ states, obtained by numerical minimization of the Ginzburg-Landau free energy functional. The magnetization only has the component perpendicular to the superconducting plane. Here $\alpha_0 = -1$, $\beta_i = 1$, $\gamma_2 = 0.5$, $m_1 = m_c = 1$ and $m_2 = 2$. We consider a weak defect with $\tilde{\alpha}_i = 0.1$ and $r_0 = 1.5$.

We see that B scales linearly with δ_i and, hence, with the defect potential $\tilde{\alpha}_i(r)$. For $\tilde{\alpha}_i = \tilde{\alpha} \cos(n\theta)$, the magnetic field $\mathbf{B}(\mathbf{r})$ behaves as

$$\mathbf{B}(\mathbf{r}) \propto \tilde{\alpha} \left[B_1(r) \sin\left[(n+2)\theta\right] + B_2(r) \sin\left[(n-2)\theta\right] \right] \hat{z}, \quad (13)$$

The angular dependence is obviously different from that in an $s + is$ state [see Eq. (7)]. The right-hand side of Eq. (12) is presented in explicit form in Eq. (A10), and the functions $B_i(r)$ are obtained by substituting (A10) into (12) and solving
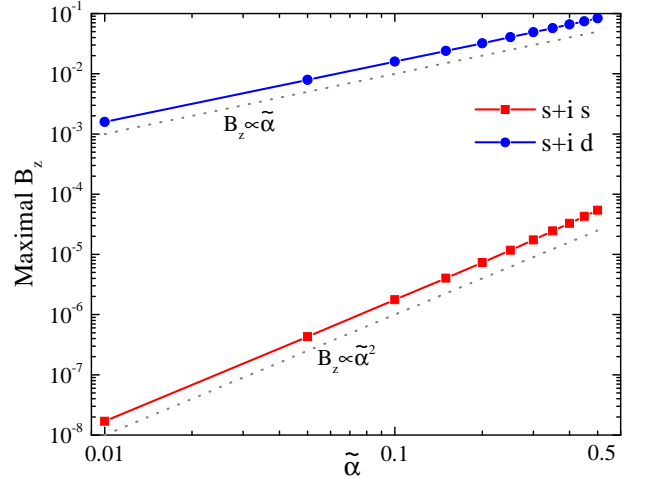

FIG. 3. (color online) Maximal magnetization field induced by a square defect in the $s + is$ and $s + id$ states. Symbols are numerical results and lines are guide to eyes. The parameters are the same as those in Fig. 2 but with a different strength of the defect potential. The magnetization is in unit of $H_{c2} = \Phi_0/2\pi\xi_1^2$ with ξ_1 being the coherence length of the first band.
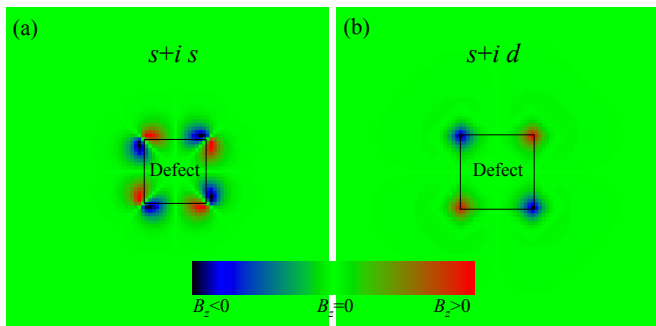
FIG. 4. (color online) Spontaneous magnetization induced by a square defect in the $s + is$ and $s + id$ states. The magnetization only has the component perpendicular to the superconducting plane. Here $\alpha_0 = -1, \beta_i = 1, \gamma_2 = 0.5, m_1 = m_c = 1$ and $m_2 = 2$. The strength of the defect potential is $\tilde{\alpha}_i = 0.5$ and $r_0 = 1$.

the differential equation.

III. NUMERICAL CALCULATIONS

To complement the analytical analysis we now perform numerical minimization of $\mathcal{F}$ using time-dependent Ginzburg-Landau equations

$$\frac{\hbar^2}{2m_j D_j}(\partial_t + i\frac{2e}{\hbar}\Phi)\Psi_j = -\frac{\delta\mathcal{F}}{\delta\Psi_j^*}, \qquad (14)$$

$$\frac{\sigma}{c}(\frac{1}{c}\partial_t\mathbf{A} + \nabla\Phi) = -\frac{\delta\mathcal{F}}{\delta\mathbf{A}}, \qquad (15)$$

where D_j is the diffusion constant, σ is the normal state conductivity, and Φ is the electric potential. The details of the numerical calculations can be found in Ref. 46.

We model a defect at a point $\mathbf{r} = 0$ by setting $\alpha_i(\mathbf{r}) = \alpha_0 + \tilde{\alpha}$ for $r < r_0|\cos(n\theta)|$ and $\alpha_i(\mathbf{r}) = \alpha_0$ otherwise. The results of the calculation of the induced magnetization for various n are displayed in Fig. 2. For $n = 0$, there is no spontaneous magnetization in an $s + is$ state, while in a $s + id$ state the magnetization is non-zero and displays a two-fold angular variation. For $n > 0$, the magnetization in an $s + is$ state displays a $2n$-fold variation, consistent with the result of the linear response theory. In an $s + id$ state the induced magnetization predominantly displays the 4-fold variation for for $n = 2$ and the 2-fold variation for $n = 4$.

In Fig. 3 we show the amplitude of the induced magnetization B_z as a function of the strength of the defect potential $\tilde{\alpha}$ for a square defect. The amplitude increases linearly with $\tilde{\alpha}$ for an $s + id$ state and quadratically in an $s + is$ state, in full agreement with the analytical results.

We also analyzed a square defect with $\alpha_i(\mathbf{r}) = \alpha_0 + \tilde{\alpha}$ if $-r_0 \leq x, y \leq r_0$ and $\alpha_i(\mathbf{r}) = \alpha_0$ otherwise (see Fig. 4). The induced magnetization emerges at the corners of the square defect. It has dominant 2-fold (4-fold) angular dependence for an $s + id$ ($s + is$) state. The magnetization pattern in an $s + is$ state has C_4 rotation symmetry, while in an $s + id$ state

it is invariant under the combination of C_4 rotation and time reversal operation.

IV. RELATION TO PREVIOUS WORK

Let us compare our results to the previous work. For a circular defect, our results are consistent with those in Ref. 42 for an $s + id$ state and in Ref. 43 for an $s + is$ state. In Ref. 43 it was argued that, to linear order in defect potential, for an $s + is$ superconductor with isotropic impurities, no spontaneous supercurrent (and thus no induced magnetization) appears unless the C_4 symmetry and the time reversal symmetry are both broken. In the present work we extend that result and show that an induced magnetization can also appear in an $s + is$ superconductor even if C_4 rotation symmetry is preserved: this requires the defect to break rotational symmetry and perturbative calculations to second order in the defect potential. If the C_4 rotation symmetry is explicitly broken by a defect, an induced magnetization appears already at the first order in a defect potential.[43]

V. SUMMARY

To summarize, in this paper we have studied the emergence of a spontaneous magnetization induced by a nonmagnetic defect in a superconductor with either an $s + is$ or an $s + id$ pairing symmetry. We found that the angular dependence of a magnetization depends on the shape of a defect potential and is different for $s + is$ and $s + id$ states. For a weak defect, an induced magnetization for an $s + id$ state is linear in defect potential, while for an $s + is$ state it is quadratic. For a defect with an n-fold angular variation, the magnetization displays a $2n$-fold angular variation for an $s + is$ state and $n \pm 2$-fold angular variation for an $s + id$ state. Our results show that $s + is$ and $s + id$ pairing symmetries can be distinguished experimentally by measuring angular dependences of the magnetization patterns.

The induced magnetization is weak (a few Gauss for a strong defect potential), but is within the resolution of several imaging methods, such as magnetic force microscope and superconducting quantum interference device, and muon-spin relaxation experiments. The shapes of the defects can be controlled by focused ion beam milling. For atomic defects, a superconducting order parameter in a spatially isotropic state is suppressed in a circular region with a radius of the order of superconducting coherence length. As a result, no spontaneous magnetization is induced by atomic defects in an $s + is$ state. Because of this, we believe that the fact that a spontaneous magnetization has not been detected in zero-field muon-spin relaxation studies of polycrystalline samples of $Ba_{1-x}K_xFe_2As_2$ with $0.5 \leq x \leq 0.9$ in Ref. 41 does not actually rule out $s + is$ pairing symmetry. We hope that future experiments with controlled shape of the defects will be able to resolve the issue whether superconductivity in $Ba_{1-x}K_xFe_2As_2$ breaks time-reversal symmetry near $x = 1$ and, if yes, whether the superconducting state is $s + is$ or $s + id$.

Appendix A: Calculations of the order parameters

Here we calculate the variations of the superconducting order parameters in the presence of a weak defect. For the $s + is$ state, the Ginzburg-Landau equations after minimizing $\mathcal{F}$ in Eq. (1) with respect to Ψ_i^* is

$$\alpha_1 \Psi_1 + \beta_1 |\Psi_1|^2 \Psi_1 - \frac{\hbar^2}{2m_1}\nabla^2\Psi_1 - \frac{\hbar^2}{4m_c}\nabla^2\Psi_2 + \gamma_2\Psi_1^*\Psi_2^2 = 0, \quad (A1)$$

$$\alpha_2 \Psi_2 + \beta_2 |\Psi_2|^2 \Psi_2 - \frac{\hbar^2}{2m_2}\nabla^2\Psi_2 - \frac{\hbar^2}{4m_c}\nabla^2\Psi_1 + \gamma_2\Psi_2^*\Psi_1^2 = 0, \quad (A2)$$

where we have set $\gamma_1 = \gamma_3 = 0$ for simplicity. Here we require $\gamma_2 > 0$ to stabilize the $s + is$ state. We have also neglected the variation of the gauge field by setting $\mathbf{A} = 0$ because the fluctuations of $\mathbf{A}$ have the gap of the superconducting gap, while the fluctuations of Ψ_i have a smaller gap in the vicinity of the time reversal symmetry breaking transition.[15,16] For a weak defect potential $\alpha_i \to \alpha_i + \tilde{\alpha}_i$ with $|\tilde{\alpha}_i| \ll |\alpha_i|$, the change of the order parameter $\Psi_i = \Psi_{i0}(1 + \delta_i + i\phi_i)$ is

$$\alpha_1 \Psi_{10}(\delta_1 + i\phi_1) + \beta_1 \left|\Psi_{10}^2\right|\Psi_{10}(3\delta_1 + i\phi_1)$$
$$-\frac{\hbar^2\Psi_{10}}{2m_1}\nabla^2(\delta_1 + i\phi_1) - \frac{\hbar^2\Psi_{20}}{4m_c}\nabla^2(\delta_2 + i\phi_2)$$
$$+\gamma_2\Psi_{10}^*\Psi_{20}^2(\delta_1 + 2\delta_2 - i\phi_1 + 2i\phi_2) = -\tilde{\alpha}_1, \quad (A3)$$

and similarly for the second component. By separating the real and imaginary parts, we obtain four linear equations for

δ_i and ϕ_i. We assume $\tilde{\alpha}_i(\mathbf{r}) = \tilde{\alpha}_i(r)\cos(n\theta)$ in the polar coordinate. The Fourier transform is $\tilde{\alpha}_i(k) = \int \tilde{\alpha}_i(r)J_n(kr)rdr$, where J_n is the Bessel function of the first kind. In the momentum space, we need to replace $\nabla^2 \to -k^2$ in Eq. (A3). By solving Eq. (A3) we find $\delta_i(k)$ and $\phi_i(k)$. By taking the inverse Fourier transform, we obtain $\delta_i(\mathbf{r}) = \cos(n\theta)\int \delta_i(k)J_n(kr)kdk$ and similarly for $\phi_i(\mathbf{r})$. For identical two band superconductors with $\alpha_i = \alpha$, $\beta_i = \beta$, $m_i = m$ and $\tilde{\alpha}_i = \tilde{\alpha}$, we have

$$\delta_1(k) = \delta_2(k) = \frac{8m\left(8m\alpha\gamma + k^2(-\beta + \gamma)\hbar^2\right)m_c^2\tilde{\alpha}(k)}{p}, \quad (A4)$$

$$\phi_1(k) = -\phi_2(k) = \frac{4k^2m^2(\beta - \gamma)\hbar^2m_c\tilde{\alpha}(k)}{p}, \quad (A5)$$

$$p \equiv k^4m^2(\gamma - \beta)\hbar^4$$
$$+4\left(4m\alpha - k^2\hbar^2\right)\left(8m\alpha\gamma + k^2(\gamma - \beta)\hbar^2\right)m_c^2. \quad (A6)$$

The spontaneous magnetization vanishes $\mathbf{B} = 0$ according to Eq. (6). Therefore magnetization appears only in asymmetric two band superconductors.

For the $s + id$ state, we need to replace $\nabla^2 \to \partial_x^2 - \partial_y^2$ in the mixed gradient term in Eqs. (A1), (A2) and (A3). In the limit $m_c \gg m_i$, we have $\phi_i = 0$. For $\alpha_i = \alpha$, $\beta_i = \beta$ and $\tilde{\alpha}_i = \tilde{\alpha}$, but $m_1 \neq m_2$, we obtain

$$\delta_1(k) = \frac{2\tilde{\alpha}(k)m_1\left(k^2(\beta - \gamma)\hbar^2 - 4\alpha(\beta + \gamma)m_2\right)}{f}, \quad (A7)$$

$$\delta_2(k) = -\frac{2\tilde{\alpha}(k)\left(k^2(-\beta + \gamma)\hbar^2 + 4\alpha(\beta + \gamma)m_1\right)m_2}{f}, \quad (A8)$$

$$f \equiv k^4(-\beta + \gamma)\hbar^4 + 4k^2\alpha\beta\hbar^2m_2$$
$$+4\alpha m_1\left(k^2\beta\hbar^2 - 4\alpha(\beta + \gamma)m_2\right). \quad (A9)$$

Denote $\delta_1(\mathbf{r}) - \delta_2(\mathbf{r}) = g(r)\cos(n\theta)$, we have

$$\partial_{x,y}(\delta_1 - \delta_2) = n\cos(2\theta)\sin(n\theta)(g - r\partial_r g)$$
$$+\frac{\sin(2\theta)\cos(n\theta)}{2}\left(n^2 g + r\left(-\partial_r g + r\partial_r^2 g\right)\right). \quad (A10)$$

From Eq. (12), we obtain the angular dependence of $\mathbf{B}$ in Eq. (13).

[1] I. I. Mazin, D. J. Singh, M. D. Johannes, and M. H. Du, "Unconventional superconductivity with a sign reversal in the order parameter of lafeaso$_{1-x}$f$_x$," Phys. Rev. Lett. **101**, 057003 (2008).

[2] Kazuhiko Kuroki, Seiichiro Onari, Ryotaro Arita, Hidetomo Usui, Yukio Tanaka, Hiroshi Kontani, and Hideo Aoki, "Unconventional pairing originating from the disconnected fermi surfaces of superconducting LaFeAsO$_{1-x}$F$_x$," Phys. Rev. Lett. **101**, 087004 (2008).

[3] D. Parker, O. V. Dolgov, M. M. Korshunov, A. A. Golubov, and

I. I. Mazin, "Extended $s_\pm$ scenario for the nuclear spin-lattice relaxation rate in superconducting pnictides," Phys. Rev. B **78**, 134524 (2008).

[4] A. V. Chubukov, D. V. Efremov, and I. Eremin, "Magnetism, superconductivity, and pairing symmetry in iron-based superconductors," Phys. Rev. B **78**, 134512 (2008).

[5] Kangjun Seo, B. Andrei Bernevig, and Jiangping Hu, "Pairing symmetry in a two-orbital exchange coupling model of oxypnictides," Phys. Rev. Lett. **101**, 206404 (2008).

[6] Wei-Qiang Chen, Kai-Yu Yang, Yi Zhou, and Fu-Chun Zhang, "Strong coupling theory for superconducting iron pnictides," Phys. Rev. Lett. **102**, 047006 (2009).

[7] Hanke W. Platt C. and Thomale R., "Zero-field μsr search for a time-reversal-symmetry-breaking mixed pairing state in superconducting $Ba_{1-x}K_xFe_2As_2$," Advances in Physics **62**, 453 (2013).

[8] T. Böhm, A. F. Kemper, B. Moritz, F. Kretzschmar, B. Muschler, H.-M. Eiter, R. Hackl, T. P. Devereaux, D. J. Scalapino, and Hai-Hu Wen, "Balancing act: Evidence for a strong subdominant d-wave pairing channel in $ba_{0.6}k_{0.4}fe_2as_2$," Phys. Rev. X **4**, 041046 (2014).

[9] S. Graser, T. A. Maier, P. J. Hirschfeld, and D. J. Scalapino, "Near-degeneracy of several pairing channels in multiorbital models for the fe pnictides," New Journal of Physics **11**, 025016 (2009).

[10] S. Maiti, M. M. Korshunov, T. A. Maier, P. J. Hirschfeld, and A. V. Chubukov, "Evolution of symmetry and structure of the gap in iron-based superconductors with doping and interactions," Phys. Rev. B **84**, 224505 (2011).

[11] D. F. Agterberg, Victor Barzykin, and Lev P. Gor'kov, "Conventional mechanisms for exotic superconductivity," Phys. Rev. B **60**, 14868–14871 (1999).

[12] V. Stanev and Z. Tešanović, "Three-band superconductivity and the order parameter that breaks time-reversal symmetry," Phys. Rev. B **81**, 134522 (2010).

[13] Xiao Hu and Zhi Wang, "Stability and josephson effect of time-reversal-symmetry-broken multicomponent superconductivity induced by frustrated intercomponent coupling," Phys. Rev. B **85**, 064516 (2012).

[14] Troels Arnfred Bojesen, Egor Babaev, and Asle Sudbø, "Time reversal symmetry breakdown in normal and superconducting states in frustrated three-band systems," Phys. Rev. B **88**, 220511 (2013).

[15] Shi-Zeng Lin and Xiao Hu, "Massless leggett mode in three-band superconductors with time-reversal-symmetry breaking," Phys. Rev. Lett. **108**, 177005 (2012).

[16] Valentin Stanev, "Model of collective modes in three-band superconductors with repulsive interband interactions," Phys. Rev. B **85**, 174520 (2012).

[17] Shi-Zeng Lin, "Ground state, collective mode, phase soliton and vortex in multiband superconductors," Journal of Physics: Condensed Matter **26**, 493202 (2014).

[18] Julien Garaud, Johan Carlström, and Egor Babaev, "Topological solitons in three-band superconductors with broken time reversal symmetry," Phys. Rev. Lett. **107**, 197001 (2011).

[19] Shi-Zeng Lin and Xiao Hu, "Phase solitons in multi-band superconductors with and without time-reversal symmetry," New Journal of Physics **14**, 063021 (2012).

[20] Julien Garaud and Egor Babaev, "Domain walls and their experimental signatures in $s+is$ superconductors," Phys. Rev. Lett. **112**, 017003 (2014).

[21] M. Marciani, L. Fanfarillo, C. Castellani, and L. Benfatto, "Leggett modes in iron-based superconductors as a probe of time-reversal symmetry breaking," Phys. Rev. B **88**, 214508 (2013).

[22] F. J. Burnell, Jiangping Hu, Meera M. Parish, and B. Andrei Bernevig, "Leggett mode in a strong-coupling model of iron arsenide superconductors," Phys. Rev. B **82**, 144506 (2010).

[23] Saurabh Maiti and Andrey V. Chubukov, "$s+is$ state with broken time-reversal symmetry in fe-based superconductors," Phys. Rev. B **87**, 144511 (2013).

[24] Johan Carlström, Julien Garaud, and Egor Babaev, "Length scales, collective modes, and type-1.5 regimes in three-band superconductors," Phys. Rev. B **84**, 134518 (2011).

[25] Mihail Silaev, Julien Garaud, and Egor Babaev, "Unconventional thermoelectric effect in superconductors that break time-reversal symmetry," Phys. Rev. B **92**, 174510 (2015).

[26] Julien Garaud, Mihail Silaev, and Egor Babaev, "Thermoelectric signatures of time-reversal symmetry breaking states in multiband superconductors," Phys. Rev. Lett. **116**, 097002 (2016).

[27] H. Ding, P. Richard, K. Nakayama, K. Sugawara, T. Arakane, Y. Sekiba, A. Takayama, S. Souma, T. Sato, T. Takahashi, Z. Wang, X. Dai, Z. Fang, G. F. Chen, J. L. Luo, and N. L. Wang, "Observation of fermi-surfacedependent nodeless superconducting gaps in $Ba_{0.6}K_{0.4}Fe_2As_2$," EPL (Europhysics Letters) **83**, 47001 (2008).

[28] K. Nakayama, T. Sato, P. Richard, Y.-M. Xu, T. Kawahara, K. Umezawa, T. Qian, M. Neupane, G. F. Chen, H. Ding, and T. Takahashi, "Universality of superconducting gaps in overdoped $Ba_{0.3}K_{0.7}Fe_2As_2$ observed by angle-resolved photoemission spectroscopy," Phys. Rev. B **83**, 020501 (2011).

[29] R. Khasanov, D. V. Evtushinsky, A. Amato, H.-H. Klauss, H. Luetkens, Ch. Niedermayer, B. Büchner, G. L. Sun, C. T. Lin, J. T. Park, D. S. Inosov, and V. Hinkov, "Two-gap superconductivity in $Ba_{1-x}K_xFe_2As_2$: A complementary study of the magnetic penetration depth by muon-spin rotation and angle-resolved photoemission," Phys. Rev. Lett. **102**, 187005 (2009).

[30] X. G. Luo, M. A. Tanatar, J.-Ph. Reid, H. Shakeripour, N. Doiron-Leyraud, N. Ni, S. L. Bud'ko, P. C. Canfield, Huiqian Luo, Zhaosheng Wang, Hai-Hu Wen, R. Prozorov, and Louis Taillefer, "Quasiparticle heat transport in single-crystalline $Ba_{1-x}K_xFe_2As_2$: Evidence for a k-dependent superconducting gap without nodes," Phys. Rev. B **80**, 140503 (2009).

[31] A. D. Christianson, E. A. Goremychkin, R. Osborn, S. Rosenkranz, M. D. Lumsden, C. D. Malliakas, I. S. Todorov, H. Claus, D. Y. Chung, M. G. Kanatzidis, R. I. Bewley, and T. Guidi, "Unconventional superconductivity in $Ba_{0.6}K_{0.4}Fe_2As_2$ from inelastic neutron scattering," Nature **456**, 930–932 (2008).

[32] T. Sato, K. Nakayama, Y. Sekiba, P. Richard, Y.-M. Xu, S. Souma, T. Takahashi, G. F. Chen, J. L. Luo, N. L. Wang, and H. Ding, "Band structure and fermi surface of an extremely overdoped iron-based superconductor KFe_2As_2," Phys. Rev. Lett. **103**, 047002 (2009).

[33] K. Okazaki, Y. Ota, Y. Kotani, W. Malaeb, Y. Ishida, T. Shimojima, T. Kiss, S. Watanabe, C.-T. Chen, K. Kihou, C. H. Lee, A. Iyo, H. Eisaki, T. Saito, H. Fukazawa, Y. Kohori, K. Hashimoto, T. Shibauchi, Y. Matsuda, H. Ikeda, H. Miyahara, R. Arita, A. Chainani, and S. Shin, "Octet-line node structure of superconducting order parameter in KFe_2As_2," Science **337**, 1314–1317 (2012).

[34] Kyuil Cho, M. Konczykowski, S. Teknowijoyo, M. A. Tanatar, Y. Liu, T. A. Lograsso, W. E. Straszheim, V. Mishra, S. Maiti, P. J. Hirschfeld, and R. Prozorov, "Energy Gap Evolution Across the Superconductivity Dome in Single Crystals of $Ba_{1-x}K_xFe_2As_2$," arXiv:1605.04183 [cond-mat] (2016).

[35] J.-Ph Reid, A. Juneau-Fecteau, R. T. Gordon, S. Ren de Cotret, N. Doiron-Leyraud, X. G. Luo, H. Shakeripour, J. Chang, M. A. Tanatar, H. Kim, R. Prozorov, T. Saito, H. Fukazawa, Y. Kohori, K. Kihou, C. H. Lee, A. Iyo, H. Eisaki, B. Shen, H.-H. Wen, and Louis Taillefer, "From d-wave to s-wave pairing in the iron-pnictide superconductor (Ba, K)Fe_2As_2," Superconductor Science and Technology **25**, 084013 (2012).

[36] J.-Ph. Reid, M. A. Tanatar, A. Juneau-Fecteau, R. T. Gordon, S. René de Cotret, N. Doiron-Leyraud, T. Saito, H. Fukazawa, Y. Kohori, K. Kihou, C. H. Lee, A. Iyo, H. Eisaki, R. Prozorov, and Louis Taillefer, "Universal heat conduction in the iron arsenide superconductor KFe_2As_2: Evidence of a d-wave state," Phys. Rev. Lett. **109**, 087001 (2012).

[37] F. F. Tafti, A. Juneau-Fecteau, M.- Delage, S. Ren de Cotret, J.-Ph

Reid, A. F. Wang, X.-G. Luo, X. H. Chen, N. Doiron-Leyraud, and Louis Taillefer, "Sudden reversal in the pressure dependence of Tc in the iron-based superconductor KFe$_2$As$_2$," Nature Physics 9, 349–352 (2013).

[38] F. F. Tafti, J. P. Clancy, M. Lapointe-Major, C. Collignon, S. Faucher, J. A. Sears, A. Juneau-Fecteau, N. Doiron-Leyraud, A. F. Wang, X.-G. Luo, X. H. Chen, S. Desgreniers, Young-June Kim, and Louis Taillefer, "Sudden reversal in the pressure dependence of T_c in the iron-based superconductor CsFe$_2$As$_2$: A possible link between inelastic scattering and pairing symmetry," Phys. Rev. B 89, 134502 (2014).

[39] Ronny Thomale, Christian Platt, Werner Hanke, and B. Andrei Bernevig, "Mechanism for explaining differences in the order parameters of feas-based and fep-based pnictide superconductors," Phys. Rev. Lett. 106, 187003 (2011).

[40] Christian Platt, Carsten Honerkamp, and Werner Hanke, "Pairing in the iron arsenides: a functional rg treatment," New Journal of Physics 11, 055058 (2009).

[41] Z. Lotfi Mahyari, A. Cannell, C. Gomez, S. Tezok, A. Zelati, E. V. L. de Mello, J.-Q. Yan, D. G. Mandrus, and J. E. Sonier, "Zero-field μsr search for a time-reversal-symmetry-breaking mixed pairing state in superconducting Ba$_{1-x}$K$_x$Fe$_2$As$_2$," Phys. Rev. B 89, 020502 (2014).

[42] Wei-Cheng Lee, Shou-Cheng Zhang, and Congjun Wu, "Pairing state with a time-reversal symmetry breaking in feas-based superconductors," Phys. Rev. Lett. 102, 217002 (2009).

[43] Saurabh Maiti, Manfred Sigrist, and Andrey Chubukov, "Spontaneous currents in a superconductor with $s + is$ symmetry," Phys. Rev. B 91, 161102 (2015).

[44] Julien Garaud, Mihail Silaev, and Egor Babaev, "Microscopically derived multi-component Ginzburg-Landau theories for $s + is$ superconducting state," arXiv:1601.02227 (2016).

[45] Alberto Hinojosa, Rafael M. Fernandes, and Andrey V. Chubukov, "Time-reversal symmetry breaking superconductivity in the coexistence phase with magnetism in Fe pnictides," Phys. Rev. Lett. 113, 167001 (2014).

[46] Shi-Zeng Lin and Xiao Hu, "Vortex states and the phase diagram of a multiple-component ginzburg-landau theory with competing repulsive and attractive vortex interactions," Phys. Rev. B 84, 214505 (2011).